AUTHOR QUERY FORM

ELSEVIER	**Journal: CSI** **Article Number: 2686**	**Please e-mail or fax your responses and any corrections to:** **E-mail: corrections.esil@elsevier.spitech.com** **Fax: +1 61 9699 6721**

Dear Author,

Any queries or remarks that have arisen during the processing of your manuscript are listed below and highlighted by flags in the proof. Please check your proof carefully and mark all corrections at the appropriate place in the proof (e.g., by using on-screen annotation in the PDF file) or compile them in a separate list.

For correction or revision of any artwork, please consult http://www.elsevier.com/artworkinstructions.

Articles in Special Issues: Please ensure that the words 'this issue' are added (in the list and text) to any references to other articles in this Special Issue.

Uncited references: References that occur in the reference list but not in the text – please position each reference in the text or delete it from the list.

Missing references: References listed below were noted in the text but are missing from the reference list – please make the list complete or remove the references from the text.

Location in article	Query / remark Please insert your reply or correction at the corresponding line in the proof
Q1	Please provide date of publication.
Q2	Please provide date of publication.
Q3	Please provide date of publication.
Q4	Please provide the following: volume number, issue details, and pagination information here.

Electronic file usage

Sometimes we are unable to process the electronic file of your article and/or artwork. If this is the case, we have proceeded by:

☐ Scanning (parts of) your article ☐ Rekeying (parts of) your article ☐ Scanning the artwork

Thank you for your assistance.

Computer Standards & Interfaces xxx (2009) xxx–xxx

Contents lists available at ScienceDirect

Computer Standards & Interfaces

journal homepage: www.elsevier.com/locate/csi

Electromagnetic characterization of chiral auxetic metamaterials for EMC applications

R. Ciobanu [a], R. Damian [a,*], I. Casian-Botez [b]

[a] Faculty of Electrical Engineering, Technical University of Iasi, Romania
[b] Faculty of Electronics and Telecommunications, Technical University of Iasi, Romania

ARTICLE INFO

Available online xxxx

Keywords:
Metamaterials
Chiral
Honeycomb
Microwave absorption

ABSTRACT

A new class of auxetic materials, a hexachiral honeycomb structure with good mechanical properties, is investigated through computer simulation and measurement. The electromagnetic properties for shielding applications are taken into account. This new material shows some interesting EMC properties (e.g. −40 dB transmittance at 2.4 GHz) and promises better performance using different insertion techniques.

1. Introduction

In the past years, an increasing amount of effort has been invested in the development of new materials, with good mechanical properties, low weight and low cost. In particular auxetic materials benefit from their negative Poisson's ratio [1] and are investigated closely in the last decade [2–4]. In the same time, we witness an increase in the electromagnetic pollution of the spectrum especially in the free bands (2.4 GHz). Coding techniques have been developed to ensure the "peaceful" coexistence of multiple emitter/receiver pairs in the same frequency band. In some cases, these techniques are not sufficient, especially when good shielding for an enclosure is imperative (aeronautics [5], medicine etc.). A natural step forward is to investigate the electromagnetic properties of these materials, in order to provide good electromagnetic shielding.

Electromagnetic metamaterials are defined [6] as artificial effectively homogeneous electromagnetic structures with unusual properties not readily available in nature. An effectively homogeneous structure is a structure whose structural average cell size p is much smaller than the guided wavelength λ_g. ie. The average cell size should be at least smaller than a quarter of wavelength,

$$p < \frac{\lambda_g}{4}. \tag{1}$$

The condition (1) is known as the effective-homogeneity limit or effective-homogeneity condition, and ensures that refractive phenomena will dominate over scattering/diffraction phenomena when a wave propagates inside the medium.

The chiral panels under test are specific metamaterials. Chirality is defined by geometry [7]. An object is called chiral if it cannot be superimposed on its mirror image by translations and rotations. It's shown in [8–10] that in the isotropic composite chiral media consisting of chiral microstructures, the constitutive relations in the frequency domain valid for time harmonic electromagnetic fields can have the form:

$$\mathbf{D} = \varepsilon_c \mathbf{E} + j\xi_c H \tag{2}$$

$$\mathbf{H} = j\xi_c \mathbf{E} + \mathbf{B} / \mu_c \tag{3}$$

where ε_c and μ_c represent the permittivity and permeability, and ξ_c, the chirality admittance, which is a measure of the handedness of the medium.

2. Computer simulation

2.1. Test details

The structure used in tests was a fiber reinforced polymer [11] prototype, developed in the framework of the CHISMACOMB (CHIral SMArt honeyCOMB) FP6-EU-013641 project [12], by Italcompany (Fig. 1). The structure is a hexachiral honeycomb, each of the equally spaced cylinders being connected to his 6 neighbors by ligaments.

In order to limit the dimensions of the model, the periodicity of the structure has been investigated. While the intrinsic unit cell for this structure will contain only one cylinder and half of every surrounding ligament, numerical electromagnetic computation demands a rectangular unit cell. The rectangular unit cell is showed in Fig. 2, the length and width being equal to $2 \cdot L$(x direction) and $L \cdot \sqrt{3} \cdot$(y direction) respectively (where L is the cylinder separation). The typical dimensions used in tests are shown in Table 1.

* Corresponding author. Facultatea de Electronica si Telecomunicatii, Bd. Carol I nr.11, Iasi, 700506, Romania. Tel.: +40 232 213737x137; fax: +40 232 217720.
E-mail address: rdamian@etc.tuiasi.ro (R. Damian).

0920-5489/$ – see front matter © 2009 Elsevier B.V. All rights reserved.
doi:10.1016/j.csi.2009.11.004

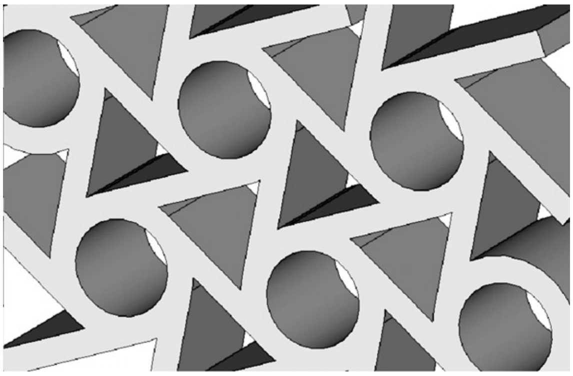

Fig. 1. Hexachiral honeycomb.

Table 1
Typical dimensions.

Parameter	Value
D	18.58 mm
h	19.75 mm
L	24.72 mm
g	3.3 mm
ε	2.5 (4)
tan δ	0 (0.1–0.5)

We investigate the interaction between a plane wave and an infinitely large sheet of auxetic material, at normal incidence. The boundary conditions are set to electric wall (x direction walls) and magnetic wall (y direction walls) in order to force the symmetry needed (plane wave) for the electromagnetic fields [13]. An input wave port is placed at some distance from the structure; the second (exit) wave port is added only when losses inside the structure are taken into account.

The results of the simulation show the S parameters for the structure. The typical shielding parameters reflectance, transmittance and absorption are related to the S parameters by the following equations [14].

$$R = |S_{11}|^2 \tag{4}$$

$$T = |S_{21}|^2 \tag{5}$$

$$A = 1-R-T = 1-|S_{11}|^2-|S_{21}|^2 \tag{6}$$

2.2. Accuracy of the results

The software tool used for the electromagnetic simulation was CST Microwave Studio 2006, which is capable to perform both FDFD (frequency domain) and FDTD (time domain) simulations. In order to verify the boundary conditions setup a three layer Jaumann microwave absorber was investigated in the same test setup. The results in Fig. 3 were found to be identical to those mentioned in [15].

For the hexachiral structure under test, the auxetic layer is illuminated with a plane wave, coming from the z direction, with normal incidence to the material. The polarization of the plane wave in the material is imposed by the electric/magnetic wall boundary conditions, and for correct calculations we expect the electromagnetic fields inside the structure to follow the characteristics of the incident wave. As in Fig. 4, we find that inside the hexachiral honeycomb, the electric field will have only E_x component, whereas the magnetic field shows only H_y component.

The final test was the comparison between the FDTD and FDFD analysis results for the same structure. The two computation methods are not related, even the mesh is different in this case (hexahedral with Perfect Boundary Approximation® — PBA for FDTD and tetrahedral for the frequency domain solver). The results are found to be essentially the same (see Fig. 5).

The difference between the two curves is maximum ± 1 dB in the $1 \div 10$ GHz range, except the frequencies around the reflection annulment, where a slight variation of the zero's frequency is detected (0.1 GHz, meaning a 1.8% difference between the two minima) around 5.8 GHz. The two solvers are independent even if they belong to the same software suite, so we can estimate a ± 2 dB general error coupled with a $\pm 2\%$ peak detection error for the rest of the simulations.

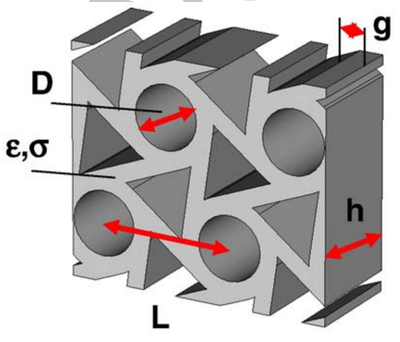

Fig. 2. Rectangular unit cell and notations used for dimensions.

2.3. Convergence stability analysis

2.3.1. Frequency domain analysis

The CST Microwave Studio frequency domain solver solves the problem for a single frequency at a time, and for a number of adaptively chosen frequency samples in the course of a frequency sweep. For each frequency sample, the linear equation system will be solved by an iterative (e.g. conjugate gradient) or sparse direct solver.

Results obtained through frequency domain analysis are plotted in Fig. 6. Seven adaptive passes were performed, the number of mesh cells increasing from 2145 to 149,328. As we see, from the 5th pass, no noticeable difference between the results is found, so in this case we have a good convergence to a solution.

2.3.2. Time domain analysis

The CST Microwave Studio time domain solver calculates the development of fields through time at discrete locations and at discrete time samples. It calculates the transmission of energy between various ports and/or open space of the investigated structure.

The fields are calculated step by step through time by the so called "Leap Frog" updating scheme. It is proven that this method remains stable if the step width for the integration does not overcome a known limit. This value of the maximum usable time step is directly related to the minimum mesh step width used in the discretization of the structure. So, the denser the chosen grid, the smaller the usable time step width.

Results obtained through FDTD analysis are plotted in Fig. 7. Ten adaptive passes were performed, the number of mesh cells increasing from 2145 to 338,496. In this case, from the 5th pass, it is clear that a solution cannot be found, all values being annulled (up to a small value $\sim 10^{-5}$ which can be attributed to round off errors). This convergence problem was corrected in CST Microwave Studio 2006B (service pack 3) but at the time we wrote this paper CST Microwave Studio 2006 was used.

Please cite this article as: R. Ciobanu, et al., Electromagnetic characterization of chiral auxetic metamaterials for EMC applications, Comput. Stand. Interfaces (2009), doi:10.1016/j.csi.2009.11.004

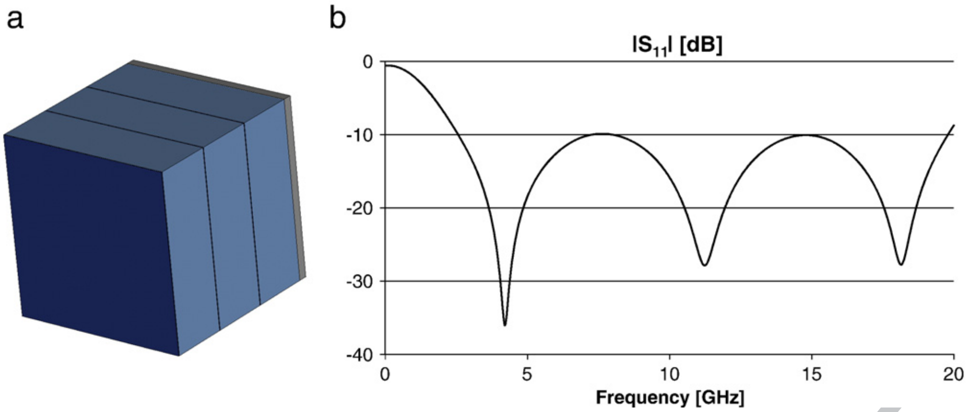

Fig. 3. Three layers Jaumann microwave absorber and results.

Both analyses (frequency and time domain) were performed with hexahedral meshing, the CST proprietary technology Perfect Boundary Approximation® (PBA) is used for the spatial discretization of the structure. The simulated structure and the electromagnetic fields are mapped to hexagonal mesh. PBA allows a very good approximation of even curved surfaces within the cubic mesh cells [16].

2.4. Computational efficiency

As Figs. 6 and 7 show, at a glance, the frequency domain solver offers better results so it would be the solver to choose in this case. However computational efficiency is to be taken into account in order to have real time solutions.

A first thing to consider is the time needed to perform the computations. Fig. 8 shows the time elapsed to the achievement of the solution. For the reference, all previous computations were made on an IBM compatible computer, with Intel Core2 E6400@2.13 GHz processor, 2 GB RAM, only one of the two separate processing cores being used by the solver.

The first thing to consider is the tremendous difference between the two solvers. The 7th pass frequency solver used 152,068 s (e.g. 42 h, 11 m, and 53 s) to achieve the solution whereas the 10th pass time domain solver only needed 91 s. When multiple analyses are to be performed (parametric studies in this paper involved more than 200 different analyses) the time consumed has a critical importance.

Another important parameter is the number of mesh cell used for the discretization of the structure. This number closely relates with the amount of memory used in computations. As mentioned before the number of mesh cells was 338,496 for the FDTD solver 10th pass, and only 149,328 for the FDFD solver 7th pass.

However it's not only the mesh cells number who decides the memory occupation. Every algorithm has its own memory consumption particularities. The time domain algorithm is more memory efficient (even at 2 times more mesh cells, less memory is used e.g. 97 MB vs. 865 MB).

2.5. Parametric analysis

Parametric studies investigated the effect of the dimensions (L, D, h, and g) and material properties (ε, σ, and $\tan\delta$). Figs. 9 and 10 show the influence of D, g, L, and h (in this order) for the lossless dielectric over the reflection coefficient (S_{11}), and Figs. 11 and 12 show the influence of ε, σ, and $\tan\delta$ over reflection coefficient (S_{11}) or over the transmission coefficient (S_{21}) when losses are taken into account (σ and $\tan\delta$).

Analysis shows that the chiral structure has almost identical properties (Figs. 9–11) with an equivalent homogeneous dielectric layer, so the mechanical and thermal advantages provided by the structure do not affect the electromagnetic properties in the bandwidth considered (0.1–10 GHz).

An interesting conclusion is the almost undetectable influence of the cylinder diameter (D) and cylinder separation (L) over the shielding properties, meaning that those parameters can be chosen strictly from mechanical and thermal considerations. Other parameters offer the

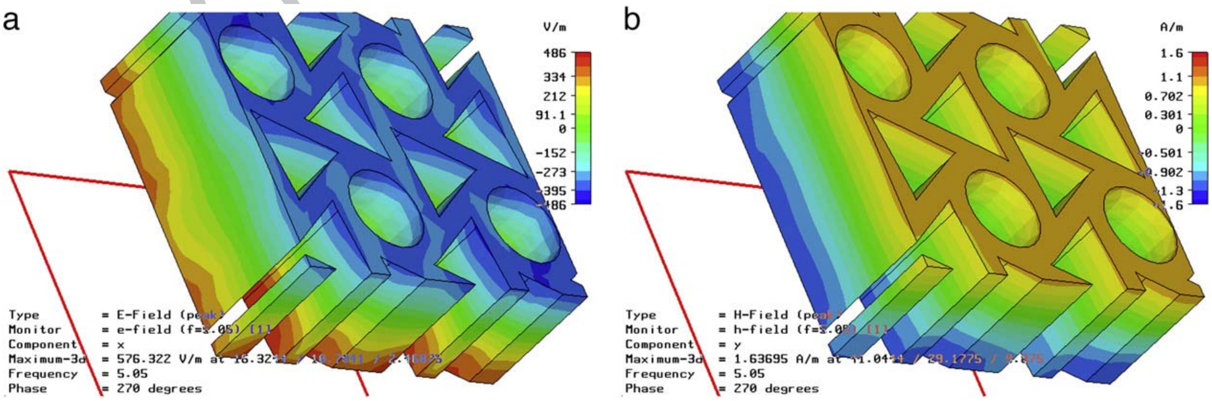

Fig. 4. E_x (left) and H_y (right) inside the structure.

Please cite this article as: R. Ciobanu, et al., Electromagnetic characterization of chiral auxetic metamaterials for EMC applications, Comput. Stand. Interfaces (2009), doi:10.1016/j.csi.2009.11.004

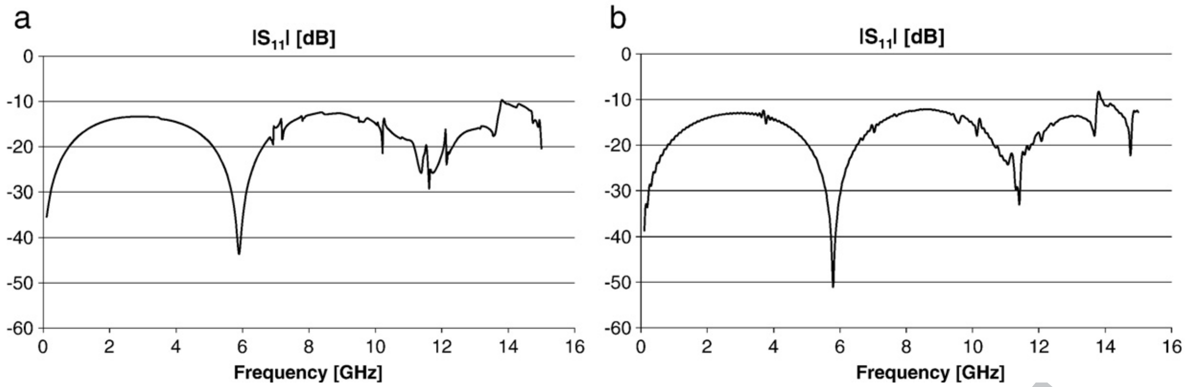

Fig. 5. S_{11} for the lossless structure by FDFD (left) and FDTD (right) computation.

expected results, e.g. lower transmission with greater losses (tan δ), increased ligament thickness (g) and the variation of the frequency of the reflection zeros with layer's height (h).

For a chiral layer (of thickness d), positioned on an ideally conducting surface, the reflection coefficient for normally incident plane waves is [7]:

$$R = \frac{\eta_M - \eta_0}{\eta_M + \eta_0} = \frac{Z_M - Z_0}{Z_M + Z_0} \tag{7}$$

where Z_M is the input impedance at the layer boundary (sometimes called the surface impedance), given by

$$Z_M = -j\sqrt{\frac{\mu_c}{\varepsilon_c}}\tan(d\omega\sqrt{\varepsilon_c \mu_c}). \tag{8}$$

In this equation ε_c and μ_c represent the usual permittivity and permeability in the formalism given by Eqs. (2) and (3). In Eq. (8) there is no dependence of the reflection coefficient on the chirality parameter, ξ_c so the results we obtain verify the existing theory. Only normal incidence on chiral media was considered, the case of oblique incidence [17] could show some influence of the microscopic structure, and must be studied further. The microscopic chirality of potential inclusions affects the values of the permittivity and permeability in Eq. (8), which then define the reflective properties, so the sparse structure of typical chiral materials offers good energy dissipation (always a “plus” for an energy absorber) and easy access for eventual FSS (Frequency Selective Surfaces) insertions inside the material in order to obtain better electromagnetic absorption. An analysis of the effective electromagnetic properties of other types of honeycomb composites is made in [18], as long as the effective-homogeneity condition (1) applies. However in [18] only the

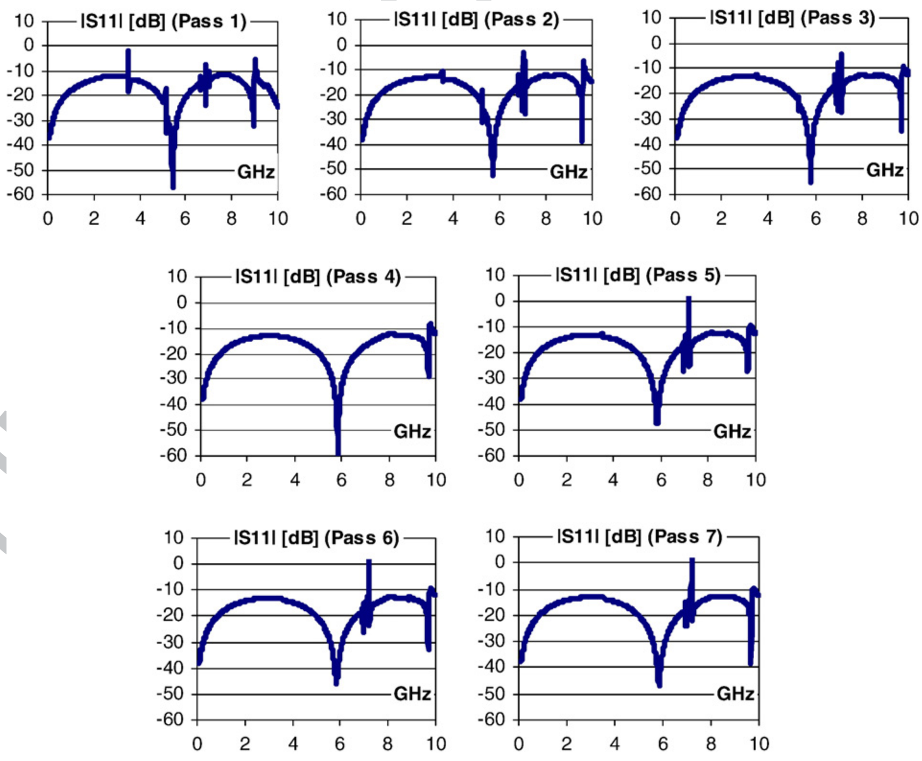

Fig. 6. $|S_{11}|$ versus frequency (passes 1 to 7, frequency domain analysis).

Please cite this article as: R. Ciobanu, et al., Electromagnetic characterization of chiral auxetic metamaterials for EMC applications, Comput. Stand. Interfaces (2009), doi:10.1016/j.csi.2009.11.004

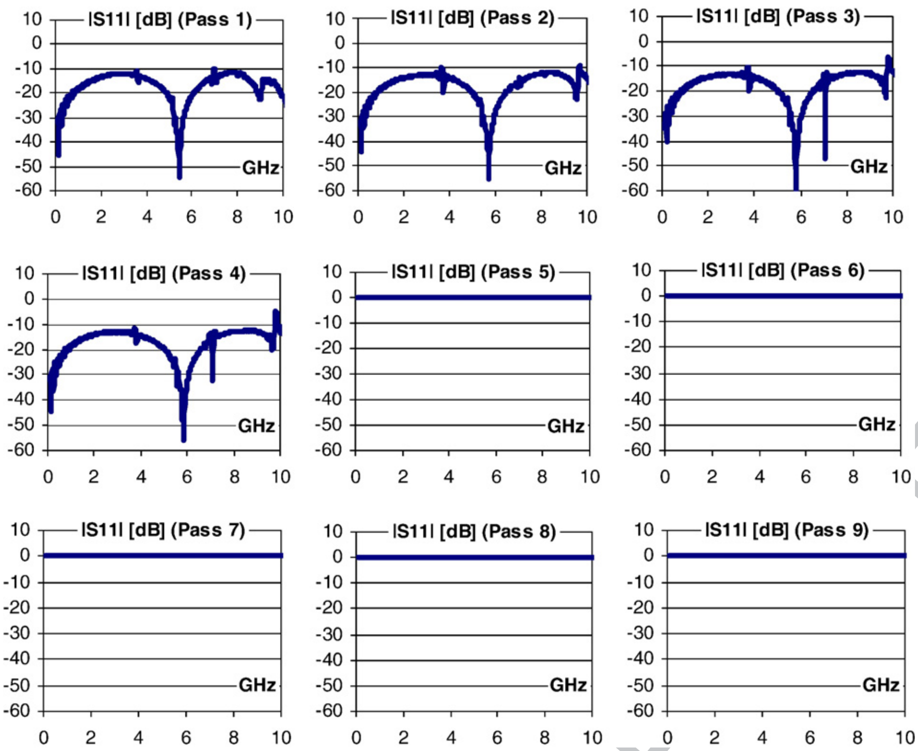

Fig. 7. $|S_{11}|$ versus frequency (passes 1 to 9, time domain analysis).

dependence of the effective electrical permittivity on the fill factor (density of the structure) was considered.

Figs. 9–11 show that for the lossless chiral layer we have a typical half-wave reflectionless slab [19]. We obtain zeroes for the reflection coefficient at the frequencies which verify the condition:

$$h = k\cdot\frac{\lambda_g}{2} = \frac{k}{2}\cdot\frac{c}{f\sqrt{\varepsilon_{eff}}} \qquad (9)$$

where k must be an integer and λ_g is the guided wavelength, inside the equivalent homogeneous dielectric slab.

This behavior offers interesting electromagnetic applications, as radar invisibility or building wall transparency. As an example we can imagine a situation where for an internal wireless network we must minimize the multiple reflections which can occur inside the building.

Eq. (9) offers the possibility to use the results in Fig. 10 to investigate the variation of the effective electrical permittivity on the frequency. Every value for layer's height (h) generate at least two minima of the reflectivity in the bandwidth considered, corresponding to $k=1$, $k=2$ in Eq. (9). We can compute the effective electrical permittivity with Eq. (10).

$$\varepsilon_{eff}(f_{min,k}) = \left(\frac{k\cdot c}{2f_{min,k}}\cdot h\right)^2 \qquad (10)$$

The effective electrical permittivity increases linearly with the frequency, as the electromagnetic field is confined inside the dielectric at higher frequency. The results in Fig. 10 on which Fig. 13 is based are obtained for $\varepsilon=2.5$ for the base material. In this case we find the effective permittivity ranging from 1.61 to 2.1, depending on the frequency. Also as the frequency increases we notice slight variations from the predicted linear increase, as the chirality of the structure becomes more and more evident.

The effects of the chirality appear as we increase the frequency, the electrical permittivity and the cylinder separation. In the typical situation (Table 1) Eq. (1) gives a frequency limit of about 2.37 GHz. Close inspection of the results (especially Fig. 11 where D and g

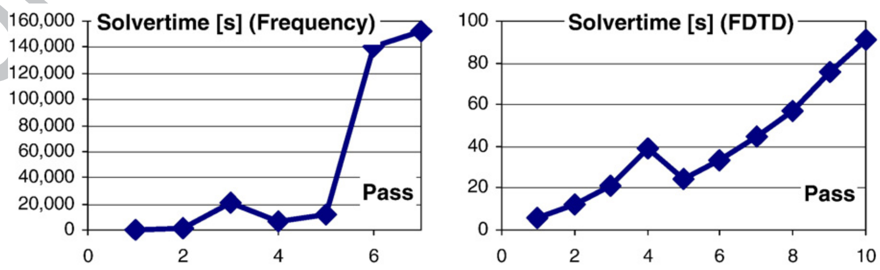

Fig. 8. Solver time versus passes — frequency (left) and time (right) domain solvers.

Please cite this article as: R. Ciobanu, et al., Electromagnetic characterization of chiral auxetic metamaterials for EMC applications, Comput. Stand. Interfaces (2009), doi:10.1016/j.csi.2009.11.004

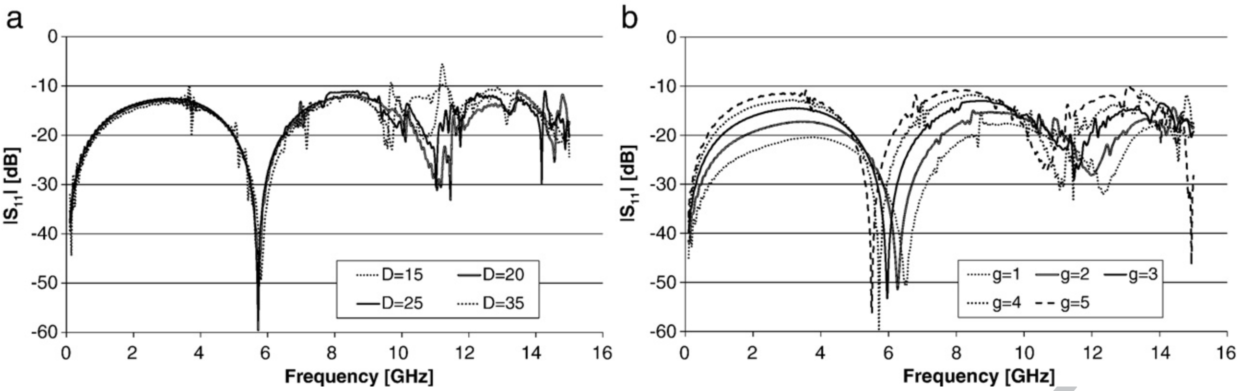

Fig. 9. Internal cylinder diameter (D — left) and ligament thickness (g — right) influence over S_{11}.

parameters have no influence over the chiral behavior) shows that obvious effects of the microscopic chiral structure are visible at 8 GHz.

Condition (1) can be expressed in terms of visible influence as:

$$L \cdot f \cdot \sqrt{\varepsilon_{\mathrm{eff}}} \approx \frac{3c}{4}. \tag{11}$$

The other results verify this relationship. Increase of ε from 2.5 to 10 (Fig. 11a) lowers the frequency of appearance of chiral effects from 8 GHz to 4 GHz (the square root of the permittivity factor of 4). Increase of L to 40 mm (Fig. 10a) shows the same effect starting from 5 GHz.

We can conclude that regarding the hexachiral honeycomb, chirality influence becomes obvious when relation (11) applies, but while visible, this influence does not affect the macroscopic behavior of the panel under test. The hexachiral panel behaves as a homogeneous dielectric, with a different effective electrical permittivity (Fig. 13), thus different methods to increase the microwave shielding capability must be applied in order to obtain an EMC capable material. Insertion of FSS or inclusion of the panels in Salisbury screen configuration could offer this result. For the measurement section of this paper we will focus on a simpler configuration, which consists in the deposition of two aluminum foils on both sides of the panel. The selected method has the advantage to have a minimal influence over

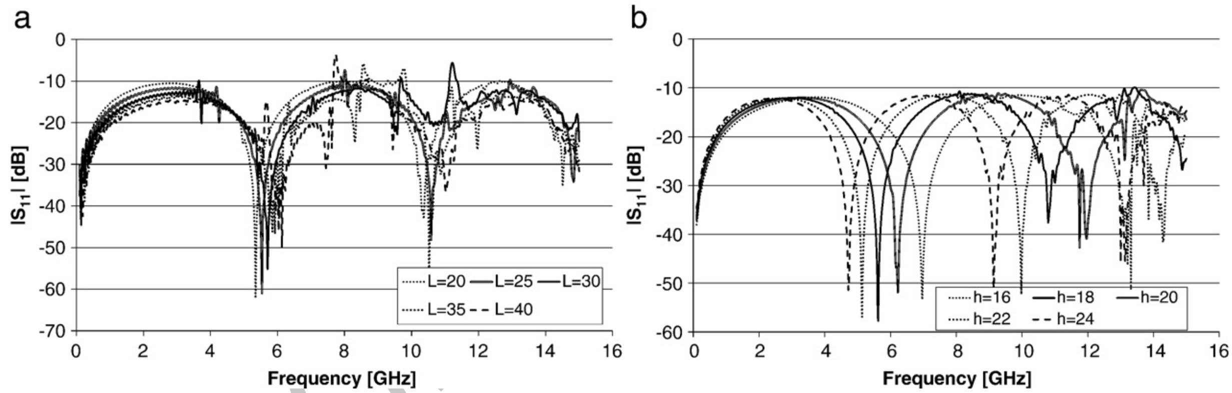

Fig. 10. Cylinder separation (L — left) and layers' height (h — right) influence over S_{11}.

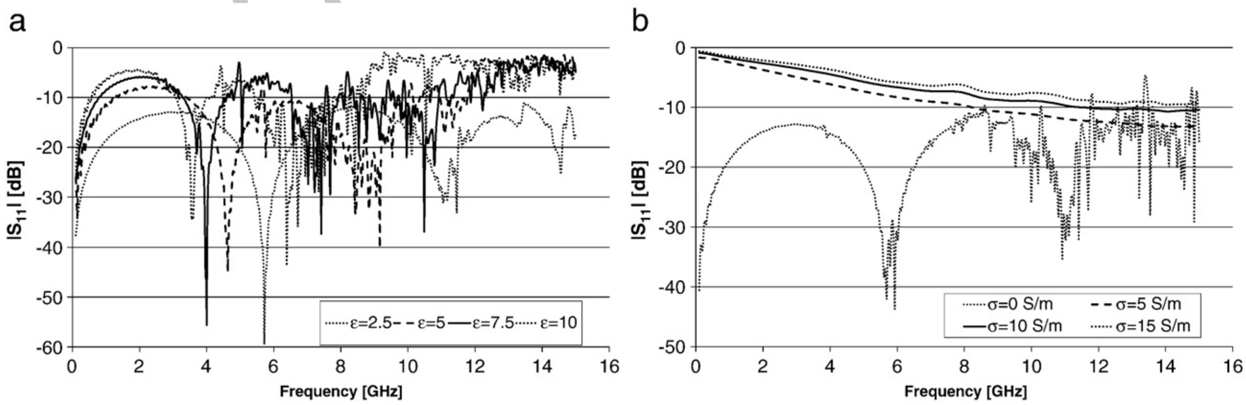

Fig. 11. Electrical permittivity (ε — left) and electric conductivity (σ — S/m — right) influence over S_{11}.

Please cite this article as: R. Ciobanu, et al., Electromagnetic characterization of chiral auxetic metamaterials for EMC applications, Comput. Stand. Interfaces (2009), doi:10.1016/j.csi.2009.11.004

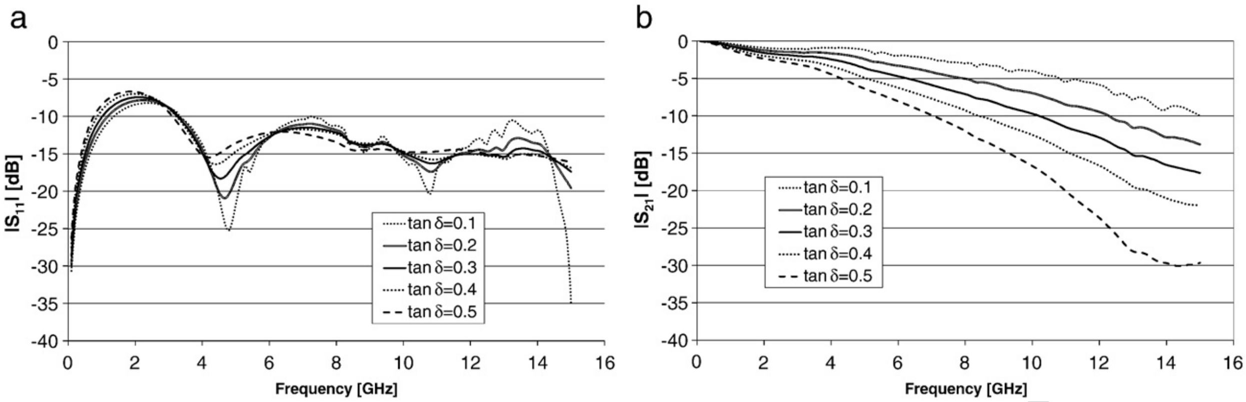

Fig. 12. Loss tangent (tan δ) influence over S_{11} (left) and S_{21} (right).

the mechanical properties of the panel (which are a key element in the CHISMACOMB Project [12]).

3. Measurements

3.1. Measurements detail

Measurements were performed using an Agilent E7405A EMC spectrum analyzer (frequency domain: 250 kHz to 40 GHz), Agilent E8257 PSG Analog Signal Generator (frequency domain: 9 kHz to 26.5 GHz), and two ETS Lindgren 3115 horn antennas (frequency domain: 1 GHz–18 GHz) in the free-space transmission measurement method (Fig. 14). Transmission simulations (Fig. 12) show that losses inserted by the intrinsic panel are in the 3–4 dB range (tan δ for the base material is around 0.01). So the intrinsic panel, equivalent from the macroscopic point of view with a homogeneous dielectric, is not suited alone for EMC applications.

In order to investigate possible microwave shielding applications, two 0.5 mm thick aluminum foils were placed on both side of the layer (Fig. 14), and the bandwidth investigated was around the free ISM band at 2.4 GHz (e.g. 1.5–3 GHz) in connection with wireless, Bluetooth or DECT telephony applications. Multiple measurements were performed with different power levels at the generator (0 dBm, −10 dBm, and −20 dBm) and were repeated seven times [20].

In order to eliminate the incertitude introduced by the quite irregular frequency characteristics of the antennas, for every frequency point, two distinct measurements were made: the first, or the reference measurement, without the probe inserted between antennas and the second, or the sample measurement, was repeated seven times with the corresponding measured sample between antennas. The value of interest will be the difference between the two measurements, as the supplemental attenuation induced by the measured sample, hence the electromagnetic shielding capability of the chiral layer with aluminum foils.

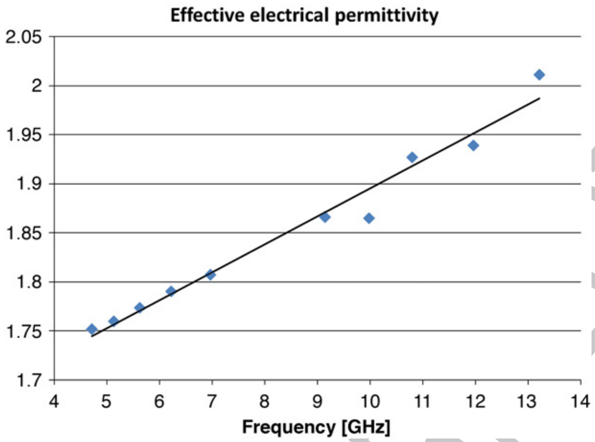

Fig. 13. Effective electrical permittivity.

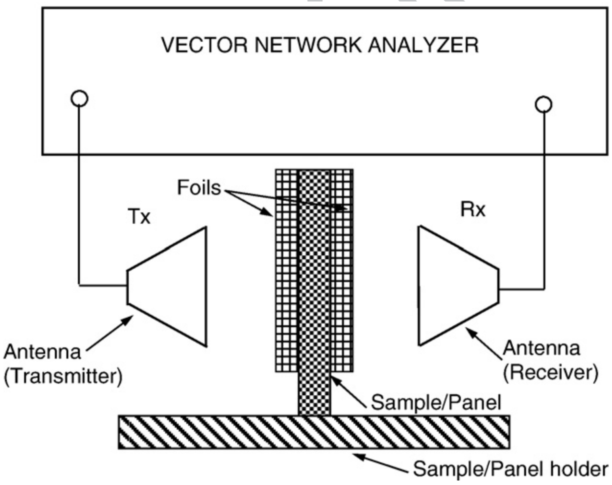

Fig. 14. Sample measurement technique.

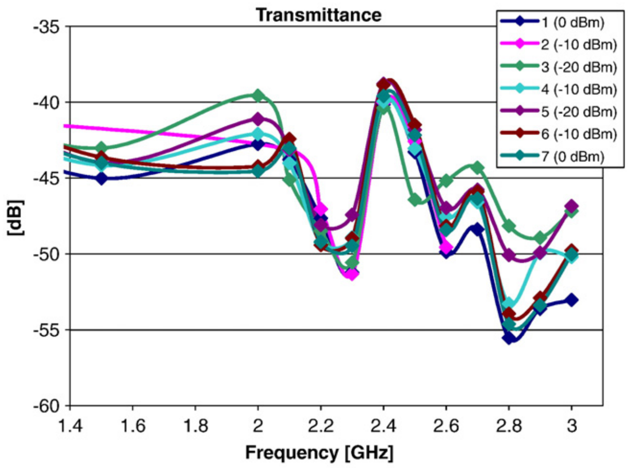

Fig. 15. Hexachiral structure transmittance.

Table 2
Measurement results and errors.

Frequency [GHz]	1.5	2	2.2	2.4	2.6	2.8	3
Transmittance [dB]	−43.97	−42.39	−48.45	−39.69	−47.96	−52.60	−49.51
Standard Deviation	0.65	1.89	0.90	0.63	1.60	2.87	2.27
Range [dB]	1.98	4.97	2.36	1.59	4.71	7.38	6.19
Meas. count	6	6	7	7	7	6	6

3.2. Measurement results

The transmittance computed from the measured transmitted power and the generator power level is plotted in Fig. 15. The measured values show good repetitive values. The transmittance at 2.4 GHz (the free bandwidth of interest) has an interesting value of −40 dB transmission (Fig. 15, Table 2) which denotes that the structure under test can clearly be used as a microwave absorber, this values being typical for a good microwave absorber [15].

Table 2 shows the statistical data for the measured values. Measurements below 1.5 GHz were omitted as the frequency range of the antennas makes them uncertain. Statistical analysis shows a measurement error ranging from 0.9 dB to 2.9 dB in higher frequencies. This precision is enough to characterize the shielding properties of the chiral panel between the two aluminum foils but certainly will not be sufficient to investigate the transmission characteristics of the simple panel (3–4 dB in the 1.5–3 GHz — Fig. 12). While better methods exists, as the coaxial holder method, which imply a sample inserted inside a waveguide, the geometrical size of the structure (mainly L) will impose a very large guide in order to include several cells. The limited bandwidth of such a waveguide (for example WR 770 in USA standard) will make any attempt to find accurate information useless.

4. Conclusions

The evaluation of the intrinsic electromagnetic properties of an auxetic material was made. We used CST Microwave Studio, for his capability to perform both frequency and time domain simulations. Particular boundary conditions (electric/magnetic walls) were used to force the electromagnetic field inside the structure to be the same as with an incident plane wave. The stability and efficiency analyses of both simulation methods were performed, showing the optimum compromise between speed and accuracy. More than 200 different structures were then analyzed in order to obtain a complete characterization of the intrinsic proprieties of the chiral metamaterial under test. The results show that the performance of the hexachiral structure is equivalent to a homogeneous dielectric layer, some of the properties being influenced by the specific geometry of the structure.

Measurements were performed in some typical microwave absorber configurations and the results show good electromagnetic shielding capacities. The same structure which offers good mechanical and thermal behaviors [21] gives access to some improvement techniques. This work will be followed by the investigation of the possibility to improve these electromagnetic properties through the use of insertions, metallization etc.

Acknowledgements

The authors gratefully acknowledge the support from the CHISMACOMB FP6-EU-013641 and PN2 ID320/2007 projects.

The authors wish to thank Mr. Tan Phu Vuong from “Laboratoire de Conception et d'Intégration des Systèmes”, ESISAR, Valence, France, for access to CST Microwave Studio 2006.

References

[1] J. Grima, Negative, negative and more negative: systems exhibiting negative Poisson's ratio, negative thermal expansion and/or negative compressibility, 4th International Workshop on Auxetics and Related Systems, Malta, 2007, p. 8.
[2] L.W. Li, D. You, M.-S. Leong, T.-S. Yeo, Electromagnetic scattering by multilayered chiral-media structures: a scattering-to-radiation transform, Journal of Electromagnetic Waves and Applications 14 (2000) 401–404.
[3] H. Ammari, M. Laouadi, J.-C. Nedelec, Low frequency behavior of solutions to electromagnetic scattering problems in chiral media, SIAM Journal of Applied Mathematics, Society for Industrial and Applied Mathematics 58 (3) (1998) 1022–1042.
[4] Rachid Oussaid, Brahim Haraoubia, Behavior of a chiral material in terms of a guided wave propagation, International Journal of Applied Electromagnetics and Mechanics 19 (2004) 631–635.
[5] D. Bornengo, F. Scarpa, C. Remillat, Evaluation of hexagonal chiral structure for morphing airfoil concept, Proceedings. IMechE, Part G: J. Aerospace Engineering, vol. 219, 2005, pp. 185–192.
[6] Christophe Caloz, Tatsuo Itoh, Electromagnetic Metamaterials: Transmission Line Theory and Microwave Applications: The Engineering Approach, John Wiley & Sons, Inc., Hoboken, New Jersey, 2006.
[7] Frederic Mariotte, Sergei A. Tretyakov, Bruno Sauviac, Modeling effective properties of chiral composites, IEEE Antennas and Propagation Magazine 38 (2) (April 1996) 22–32.
[8] Frederic Mariotte, Nader Engheta, Reflection and transmission of guided electromagnetic waves at an air–chiral interface and at a chiral slab in a parallel-plate waveguide, IEEE Transactions on Microwave Theory and Techniques 41 (11) (November 1993) 1895–1906.
[9] P. Pelet, N. Engheta, The theory of chirowaveguides, IEEE Transactions on Antennas and Propagation 38 (1) (January 1990) 90–98.
[10] M. Oksanen, P. Koivisto, S. Tretyakov, Vector circuit method applied for chiral slab waveguides, Journal of Lightwave Technology 10 (2) (February 1992) 150–155.
[11] Iqbal Ahmed Khany, S.C. Raghavendray, A.B. Kulkarni, Polyester-based chiral materials for microwave absorption applications, International Journal of Electronics 90 (3) (2003) 159–166.
[12] CHISMACOMB, A FP6 Specific Target Research Project, http://www.chismacomb.eu/. Q1
[13] CST GmbH, Application Note, Photonic Crystal Simulation, Article ID: 296, 2007 — http://www.cst.com.
[14] Y.K. Hong, C.Y. Lee, C.K. Jeong, D.E. Lee, K. Kim, J. Joo, Method and apparatus to measure electromagnetic interference shielding efficiency and its shielding characteristics in broadband frequency ranges, Review of Scientific Instruments 74 (2) (February 2003) 1098–1102.
[15] Paul Saville; Trisha Huber; Darren Makeiff — Fabrication of Organic Radar Absorbing Materials Defence R&D Canada — Atlantic, Technical Report DRDC Atlantic TR 2005-124. Q2
[16] CST of America, A software suite with total synergy, Microwave Journal 49 (1) (2006).
[17] Raymond Redheffer, The dependence of reflection on incidence angle, Ire Transactions on Microwave Theory and Techniques (October 1959) 423–429.
[18] Martin Johansson, Christopher L. Holloway, Edward F. Kuester, Effective electromagnetic properties of honeycomb composites, and hollow-pyramidal and alternating-wedge absorbers, IEEE Transactions on Antennas and Propagation 53 (2) (February 2005).
[19] Sophocles J. Orfanidis — Electromagnetic Waves and Antennas, online book, ch 5, pp. 160–166, http://www.ece.rutgers.edu/orfanidi/ewa/. Q3
[20] G. Busse, A.F. Jacob, Enhancing the range of waveguide measurement setups for chiral media by step discontinuities, International Journal of Applied Electromagnetics and Mechanics 9 (1998) 115–121.
[21] M.R. Hassan, F. Scarpa, M. Ruzzene, N.A. Mohammedd, Smart shape memory alloy chiral honeycomb, Materials Science and Engineering A (2007), doi:10.1016/j.msea.2006.10.219. Q4

Romeo-Cristian Ciobanu was born in Piatra-Neamt, Romania, in 1961. He received a Ph.D degree in Electrical Engineering from the University Politehnica of Bucharest and a Ph.D degree in Chemistry from the Technical University of Iasi.
He is currently a Professor at the Technical University of Iasi, Electrical Engineering Department. His research focuses on Industrial Diagnosis, Dielectric Measurements, Quality and Maintenance, Composite Technologies.

Radu-Florin Damian was born in Vaslui, Romania, in 1972. He received the M.Sc. and Ph.D. degree in electronic engineering from the Technical University of Iasi.
He is currently senior lecturer of microwave engineering and optoelectronics at the Technical University of Iasi, Electronics and Telecommunications Department. His research focuses on numerical electromagnetics and optoelectronics.

Irinel Casian-Botez was born in Iasi, Romania, in 1955. He received the M.Sc. degree in microwave engineering from the INP Toulouse, France, in 1992, and Ph.D. degree in electronic engineering from the Technical University of Iasi.
He spent one year with ENSEEIHT Toulouse, where he was involved in the field of time domain electromagnetics. He is currently a Professor of microwave engineering at the Technical University of Iasi. His research concerns electromagnetics and nanoelectronics.

Please cite this article as: R. Ciobanu, et al., Electromagnetic characterization of chiral auxetic metamaterials for EMC applications, Comput. Stand. Interfaces (2009), doi:10.1016/j.csi.2009.11.004